RSC Advances

ROYAL SOCIETY OF CHEMISTRY

www.rsc.org/advances

Graphic Abstract for Table of Content

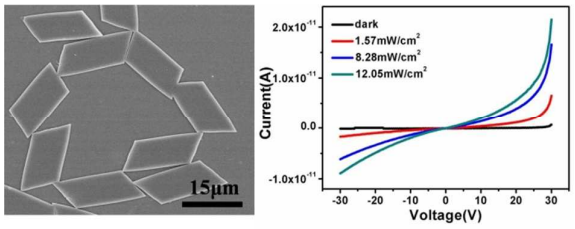

PtOEP microsheets with well-defined shape and smooth surface were fabricated, which showed active optical waveguides, photodetector and photoswitching properties.

Cite this: DOI: 10.1039/c0xx00000x

www.rsc.org/xxxxxx

ARTICLE TYPE

Facile fabrication and optoelectronic properties of platinum octaethylporphyrin microsheets

Qing-Guo Zhang,[a] Ying Lu,[a,b] Feng-Xia Wang,[b] Ying Wei*[a], Yong-Qiang Liu,[b] Bo Yang[b] and Ge-Bo Pan*[b]

Received (in XXX, XXX) XthXXXXXXXXX 20XX, Accepted Xth XXXXXXXXX 20XX
DOI: 10.1039/b000000x

Single-crystal microsheets of platinum octaethylporphyrin (PtOEP) were fabricated by a facile solution process and fully characterized. The as-fabricated microsheets had well-defined shapes and smooth surfaces, and could act as active optical waveguides. The prototype photodetector based on a single microsheet showed high reproducibility and photosensitivity with an I_{on}/I_{off} ratio of ~500.

Functional organic micro/nanostructures with controlled shapes and sizes are of great significance for miniaturized devices due to their unique physical and chemical properties.[1] Porphyrin and its derivatives have planar aromatic structures and are ideal building blocks for organic micro/nanostructures.[2,3] Previous studies have indicated that they could self-assemble into one-dimensional (1D) micro/nanostructures through π-π interaction.[3–7] The 1D products of porphyrins exhibit high thermal and chemical stabilities, and possess good electrical and optical properties.[3,6,8] However, it is noted that there are very few studies on two-dimensional (2D) micro/nanostructures of porphyrins, as well as their photoelectric properties.[2,9] The fabrication of 2D micro/nanostructures with both well-defined shapes and smooth surfaces is still a hard task for porphyrins.[10] On the other hand, 2D micro/nanostructures are expected to have different photoelectric properties from 1D ones, and are thus of great scientific interest from both fundamental and practical points of view.

Herein, we report the fabrication of micrometer-sized sheets of platinum octaethylporphyrin (PtOEP) by a facile solution process. Fig. 1a is the chemical structure of PtOEP. The targeted molecule is a typical phosphorescence material, which is extensively used in optical oxygen sensor,[11] temperature sensor,[12] organic light-emitting diode,[13] and organic solar cells.[14] Recently, 1D structures of PtOEP have been prepared by either physical vapor deposition or solution-phase precipitative method.[15,16] This differs from the present study that 2D structures of PtOEP are formed. Moreover, the as-formed microsheets are single crystals, have well-defined shapes, and can act as active optical waveguides. The prototype photodetector based on single microsheet exhibits high sensitivity, stability and photo-switching properties.

In a typical synthesis, a chloroform solution of PtOEP (2 mg/ml) was slowly injected into propylene glycol methyl ether acetate (PGMEA). The volume ratio of chloroform and PGMEA was 3:1. The mixed solution was shaken for 60s and stored at ambient conditions for ~ 3 h. Then, a drop (~ 5 μl) of PtOEP solution was deposited onto Si substrate. The solvent was allowed to evaporate completely in air and the resultant product was further annealed at 150 °C for 30 min.

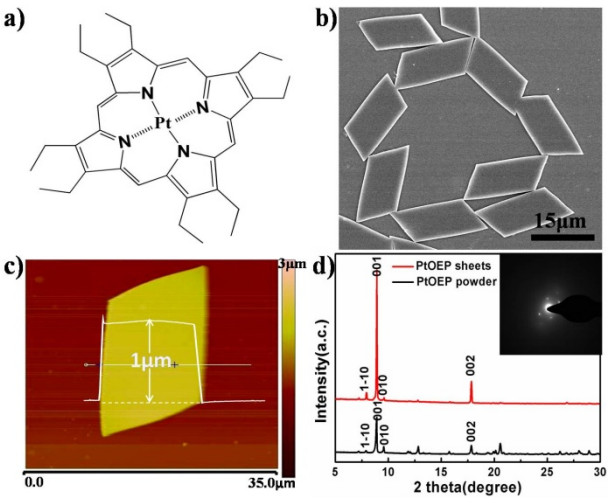

Fig. 1 (a) Chemical structure of PtOEP. (b) SEM and (c) AFM images of PtOEP microsheets. (d) XRD pattern of microsheets and source powder of PtOEP. The inset is an SAED pattern recorded within a single PtOEP microsheet.

Fig.1b shows a typical scanning electron microscopy (SEM) image of the product. The image demonstrates the formation of microsheets with well-defined shapes and smooth surfaces. The average width of microsheets is ~ 9 μm and the length is ~ 20 μm. Fig.1c shows an atomic force microscopy (AFM) image of a representative microsheet. The cross-section reveals a thickness of ~ 1 μm. It is noted that the aspect ratio (length/width) of microsheets is dependent on the volume ratio of chloroform and PGMEA. Larger aspect ratio can be obtained by increasing the PGMEA content in the mixed solution (Fig. S1, ESI†). Fig. 1d shows the XRD patterns of both microsheets and PtOEP source powder. All the diffraction peaks could be well-indexed to the triclinic phase of PtOEP.[3,16] Moreover, the diffraction peaks of (001) planes of microsheets are significantly enhanced relative to those of source powder, indicating a highly crystalline feature of microsheets. This assumption is further supported with the well-

defined SAED pattern (the inset) of a single PtOEP microsheet. In addition, the SAED pattern is consistent throughout the whole sheet, implying the single-crystalline nature of microsheet.

Fig. 2a shows the UV-vis absorption and photoluminescence (PL) spectra of microsheets and PtOEP monomers. In comparison with the monomers, the absorption bands at 382, 500, and 535 nm are broadened for microsheets. Moreover, the absorption band at 382 nm is blue-shifted to 377 nm, whereas the bands at 500 and 535 nm are red-shifted to 505 and 540 nm, respectively. The PL spectrum also reveals that the emission peak of microsheets leads to a 4 nm blue-shift compared with the monomers. The above results indicate that an ordered molecule-packing is adopted in microsheets.[3] The chemical composition of microsheets is further investigated by Fourier transform infrared (FT-IR, Fig. 2b), Raman (Fig. 2c), and energy dispersive X-ray (EDX, Fig. 2d) spectroscopy. The FT-IR spectrum of microsheets has the same feature as that of PtOEP source powder. The four characteristic bands are observed at 749, 961, 997, 1233 cm^{-1}, implying that PtOEP molecules does not undergo chemical reactions or other chemical reactions during solution process. Moreover, it is seen that the Raman spectrum (Fig.2c) of microsheets has similar features to that of PtOEP source powder. The characteristic peaks are comparable to those of PtOEP derivatives.[17] In addition, the EDX spectrum of microsheets (Fig. 2d) shows only the peaks of C, N and Pt elements, indicating that $CHCl_3$ is not involved in the PtOEP microsheets. This is consistent with the results of the FT-IR. Therefore, it is concluded that the as-fabricated microsheets are purely made of PtOEP molecules.

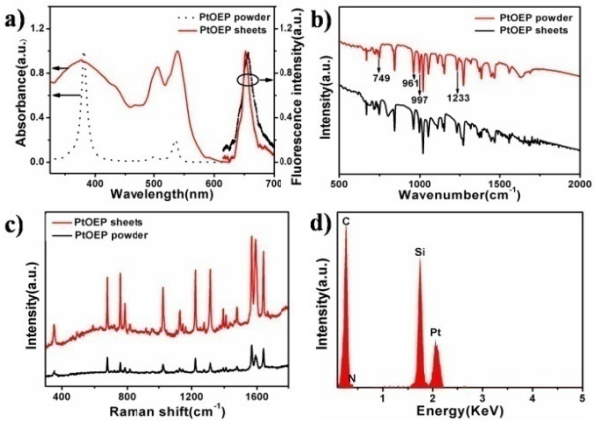

Fig. 2 (a) UV-vis absorption and PL spectra of PtOEP monomers (dot line) in chloroform and microsheets (solid line) deposited on quartz substrate. (b) FT-IR and (c) Raman spectra of microsheets and source powder of PtOEP. (d) EDX spectrum of PtOEP microsheets. The peak of Si element arises from SiO_2 substrate.

Fig. 3a represents a typical fluorescence microscopy image of a single PtOEP microsheet. It can be seen that the fluorescence intensity at the edges is stronger than that of the internal part of PtOEP microsheet. This phenomenon implies that the PtOEP microsheets can absorb the excitation light and propagate the PL emission towards the edge-interface, i.e., a typical characteristic of active waveguide is realized. In order to obtain further insight into the propagation behaviour within the microsheets, spatially resolved PL spectra of the out-coupled light with respect to the length travelled is investigated and shown in Fig. 3b. To obtain the local PL spectra, the detection tip is held at the upper terminus and the excited points are moved along the long side of a single microsheet. It can be seen that the intensities and profiles change with the detection distance. This is mainly attributed to the re-absorption of the propagation light, which is determined by the absorption behaviour of PtOEP microsheets. The above results indicate that PtOEP is a promising material used in active optical waveguides.

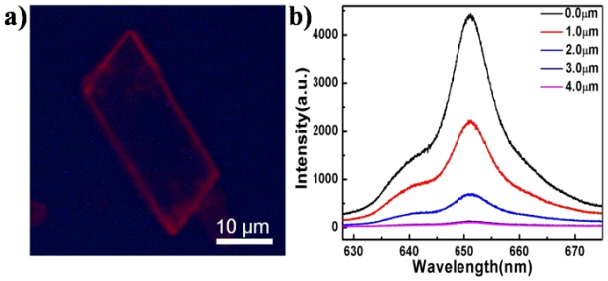

Fig. 3 (a) The fluorescence microscope image of PtOEP microsheet. (b) Spatially resolved PL spectra of the out-coupled light by excitation at a distance of 0-4 μm.

In addition, the photoresponse characteristics of microsheet are also investigated due to its excellent light absorption. Fig. 4a shows a schematic illustration of the device based on a single microsheet. Finger electrodes with the length of 200 μm, the width of 10 μm, and the distance of 10 μm are fabricated by photolithography and electron beam deposition of Au on Si substrate covered with 300 nm thick SiO_2. A drop (~5 μL) of PtOEP solution is added on the Au electrodes and the solvent is allowed to evaporate in air. To remove the solvent thoroughly, the device is annealed at 150 ^{o}C for 30 min. Fig. 4b shows a typical optical image of a real device. It can be seen that the two ends of a single PtOEP microsheet are firmly connected to two Au electrodes. The current-voltage (*I*-*V*) characteristics of devices are recorded with Keithley 4200 SCS and RF Probe Station (PE-4RF) in a clean and shielded box at room temperature. A Xenon lamp is used as the white light source. Fig. 4c shows the typical *I*–*V* curves of the device in the dark and under continuous white light illumination with varying intensity. As expected, the device exhibits obvious photoresponse characteristics. The photocurrent under light illumination is markedly higher than that obtained in the dark. At an applied bias of -20 V, the microsheet in the dark exhibits a negligible current of 0.013 pA. At a low power density of 1.57 $mWcm^{-2}$, a high current of about 1.02 pA was obtained, that is, photocurrent ratio of ~77. The photo-current/dark-current ratio is expected to be much larger if higher power illumination is employed for the photocurrent measurement. At a high power density of 12.05 $mWcm^{-2}$, the photocurrent on/off ratio can reach 375. The dependence of the photocurrent on the intensity of the incident light may lie in different photon densities from the incident light (Fig. 4c). Fig. 4d shows the relationship between the photocurrent and incident light power densities. This can be well fitted to the power law $Ip \sim P^{\theta}$, where θ determines the response of the photocurrent to the light intensity. The fitting demonstrates a power dependence of ~ 0.82, which is $I \sim P^{0.82}$, indicating the existence of quasi-uniform trap state distribution.[18]

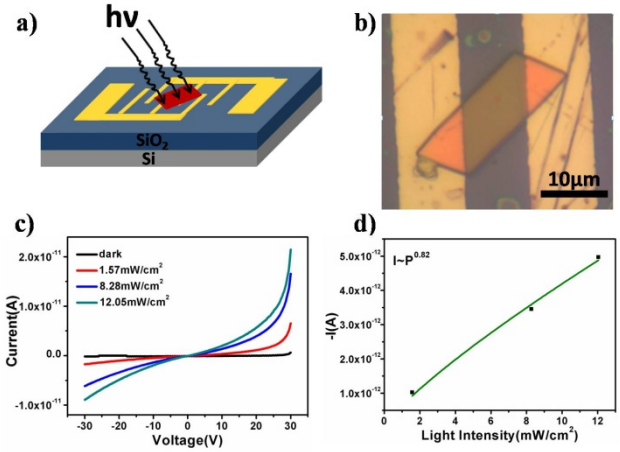

Fig. 4 (a) Schematic illustration and (b) representative optical image of device based on PtOEP microsheet. (c) Dark current and photocurrents at different incident power densities. (d) Curve of photocurrents versus incident optical densities at a bias voltage of -20 V

Moreover, the photoconduction switching is demonstrated to be prompt and reversible by light turning on and off under the illumination intensity of 12.05 mW cm^{-2} (Fig. 5a). It is clear that the current of devices increases with the bias voltage and shows two distinct states, a "low" current state in the dark and a "high" current state under white light illumination. The "on"- and "off"-state currents for 11 cycles remain almost the same. The switching in the two states is very fast and reversible, and the response time is ca. 1s from the "off"-to "on"-state, and the recovery time is ca. 1.5 s (Fig. S2, ESI†). This allows the device acting as a high-quality photosensitive switch. The excellent photoresponse characteristics may be attributed to the synergy-effect of a high orientation and charge transportability.[19] In addition, the photodetector based on the PtOEP microsheet shows high stability as shown in Fig. 5b. The photocurrent nearly holds steady and only decreases by 1.8% after 900 s illumination, indicating the high photocurrent durability of the photo detectors. A similar phenomenon has been reported in the literature and is possibly attributed to the traps and other defect states in the semiconductor nanomaterials.[20]

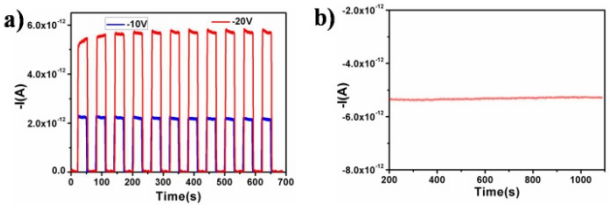

Fig. 5 (a) Time-dependent on/off switching of device based on the PtOEP microsheet. (b) Current versus time continuously over 900 s under illumination.

In summary, PtOEP microsheets with well-defined shapes and smooth surfaces were fabricated by a facile solution process. The fluorescence microscopy image and spatially resolved PL spectra of PtOEP microsheets reveal a typical characteristic of active waveguide. Moreover, the prototype photodetectors based on individual microsheets exhibit good stability, fast switching rate, and high photosensitivity. The highest ratio of I_{on}/I_{off} of the photodiode can reach 500. The superior performance together with their facile, large-scale, and low-cost preparation process makes the as-obtained PtOEP microsheets promising in waveguide sensing and photodetector devices.

This work was financially supported by the National Natural Science Foundation of China (Nos. 21273272, 21303250, 21373002, and 21003081), the National Basic Research Program of China (No. 2010CB934100), the Jiangsu Province Natural Science Foundation of China (No.BK2012192), and the Chinese Academy of Sciences.

Notes and references

[a]*Department of Chemistry, Bohai University, 121000 Jinzhou, P. R. China, Fax: 86-416-3400302; E-mail: weiying2001_77@163.com.*
[b]*Suzhou Institute of Nano-tech and Nano-bionics, Chinese Academy of Sciences, 215123 Suzhou, P. R. China, Fax: 86-512-62872663; E-mail: gbpan2008@sinano.ac.cn.*

†Electronic Supplementary Information (ESI) available: [Experimental details; SEM of PtOEP microsheets obtained at different volume ratios, the response and delay time]. See DOI:10.1039/b000000x/

1 C. Burda, X. Chen, R. Narayanan and M. El-Sayed, *Chem. Rev.*, 2005, **105**, 1025.
2 N. Chandrasekhar, S. Basak, M. Mohiddon and R. Chandrasekar, *Appl. Mater. Interfaces*, 2014, **6**, 1488.
3 H. Ji, J. Hu and L. Wan, *Chem. Commun.*, 2008, 2653.
4 T. Kojima, R. Harada, T. Nakanishi, K. Kaneko and S. Fukuzumi, *Chem. Mater.*, 2007, **19**, 51.
5 J. Hu, Y. Guo, H. Liang, L. Wan and L. Jiang, *J. Am. Chem. Soc.*, 2005, **127**, 17090.
6 F. Wang, Y. Liu, H. Wu, Y. Xiao and G. Pan, *J. Mater. Chem. C.*, 2013, **1**, 422.
7 F. Wang, Y. Liu, H. Wu and G. Pan, *Mater. Res. Express*, 2014, **1**, 1.
8 W. Campbell, A. Burrell, D. Officer and K. Jolley, *Coord. Chem. Rev.*, 2004, **248**, 1363.
9 J. Cai, H. Chen, J. Huang, J. Wang, D. Tian, H. Dong and L. Jiang, *Soft Matter.*, 2014, **10**, 2612.
10 T. Wakahara, M. Sathish, K. Miyazawa, C. Hu, Y. Tateyama, Y. Nemoto, T. Sasaki and O. Ito, *J. Am. Chem. Soc.*, 2009, **131**, 9940.
11 Y. Amao, T. Miyashitab and I. Okura, *Analyst*, 2000, **125**, 871.
12 J. Lupton, *Appl. Phys. Lett.*, 2002, **81**, 2478.
13 T. Tsuboi, M. Tanigawa, S. Kawami and T. Tsuji, *Current Applied Physics*, 2005, **5**, 633.
14 K. Xiong, L. Hou, P. Wang, Y. Xia, D. Chen and B. Xiao, *Journal of Luminescence*, 2014, **151**, 193.
15 B. Ana, A. Myriam, G. Oliver, L. Carlos and G. Pierangelo, *Chem. Mater.* , 2008, **20**, 7371.
16 M. So, V. Roy, Z. Xu, S. Chui, M. Yuen, C. Ho and C. Che, *Chem. Asian J.*, 2008, **3**, 1968.
17 B. Minaev, E. Jansson and H. Ågren, *J. Chem. Phys.*, 2006, **125**, 1.
18 S. Kung, W. Xing, W. Veer, F. Yang, K. Donavan, M. Cheng, J. Hemminger and R. Penner, *ACS Nano*, 2011, **5**, 7627
19 L. Li, P. Lee, C. Yan, T. Zhai, X. Fang, M. Liao, Y. Koide, Y. Bando and D. Golberg, *Adv. Mater.*, 2010, **22**, 5145.
20 Y. Jiang, W. Zhang, J. Jie, X. Meng, X. Fan and S. Lee., *Adv. Funct. Mater.*, 2007, **17**, 1795.